

Evaluating Wire Configurations for Tension Band Constructs using a Canine Greater Trochanteric Osteotomy Model

*Elizabeth Thompson¹ emthomp6@ncsu.edu

*Amir K. Robe² akrobe@ncsu.edu

Simon C. Roe¹ Simon_Roe@ncsu.edu

Jacqueline H. Cole² jacquecole@ncsu.edu

*Thompson & Robe are considered equal first authors as they contributed equally to the study

¹ Department of Clinical Sciences, College of Veterinary Medicine, North Carolina State University, Raleigh, NC

² Joint Department of Biomedical Engineering, University of North Carolina, Chapel Hill, NC, and North Carolina State University, Raleigh, NC

Corresponding Author: Jacqueline H. Cole
Joint Department of Biomedical Engineering
University of North Carolina and North Carolina State University
911 Oval Drive
Campus Box 7115
Raleigh, NC 27695-7115
Tel: 919-515-5955
Fax: 919-513-3814
jacquecole@ncsu.edu

Running Title: Evaluating Tension Band Wire Configurations

Author Contributions: SCR and JHC designed the experiments. AKR modified the femur model and fabricated the custom jig. ET and SCR tied the tension band wire configurations. AKR and JHC performed mechanical testing. AKR, SCR, and JHC analyzed data and made figures. ET wrote the manuscript with contributions and edits from AKR, SCR, and JHC. All authors have read and approved the final submitted manuscript.

ABSTRACT

Tension band wiring is a common fracture stabilization technique for counteracting distraction forces on a bone fragment. Previous studies optimizing performance of the tension band technique have focused on testing the overall construct, which includes the tension band configuration and K-wires or pins inserted across the fracture line. Using a metal trochanteric osteotomy model based on a canine femur, this study investigated the stability of the wire portion alone without confounding contributions of K-wire stabilization and bone stiffness. Four standard tension band configurations were applied to this model: figure-of-eight with one twist (OT) or two twists (TT), dual interlocking single loop (DISL), and double loop (DL). Configurations were mechanically tested under both monotonic and incremental cyclic loading. Initial resting tension after tying, tension remaining after each cycle, and load at 2 mm of displacement (clinical failure) were measured. The DL was the strongest and most stable configuration, generating greater resting tension, maintaining a greater percentage of resting tension under cyclic load, and resisting higher load before failure at 2 mm. Failure load was highly correlated with initial resting tension. Wire configurations that can be tightened effectively during tying, like the DL, are better able to resist the tensile load on the construct. This model for evaluating tension band wire performance could be useful to inform surgical decision-making about configuration type and tying method to achieve optimal fracture stabilization.

Keywords: tension band, fracture fixation, osteotomy, stabilization, load resistance

INTRODUCTION

The tension band (TB) technique has been in use since the 1970s as a method to resist distracting forces from a ligament or tendon on a bone fragment and convert those tensile forces into compression to help stabilize the fragment.¹⁻³ TB has been used for fixation in a variety of locations and clinical scenarios, including transpositions of the tibial tuberosity and osteotomies or fractures of the medial malleolus, distal fibula, greater trochanter, and olecranon.⁴⁻⁹ The general approach involves securing the position of the bone fragment with two K-wires or pins (depending on the size of the fragment) and placing a figure-of-eight wire opposite the direction of pull of the attached ligament or tendon to prevent bending of the pins and maintain fragment position.

Complications with TB fixation are fairly common, including migration of the K-wires, osteomyelitis, nonunion or delayed union, implant breakage, comminution of the small bone fragment, and neuropraxia.^{5,10} To reduce the rate of complications, the TB technique has been optimized through several mechanical studies examining the impact of pin and wire diameter, type of wire configuration, and osteotomy plane. In a polymer model, larger pin diameter and thicker wire resulted in stronger constructs, and the figure-of-eight configuration was stronger than a single wire loop.^{11,12} In an ulna osteotomy model, a double loop configuration resisted greater load at 2 mm of displacement compared to the standard figure-of-eight with two twists.¹³ A dual interlocking single loop configuration resisted similar loads to the standard figure-of-eight constructs. This study also showed that the wire must be placed in contact with the pins and the bone fragment to prevent fragment displacement with low loads.

Previous TB studies have incorporated a variety of configurations in the presence of K-wires with or without other securing devices, such as lag screws or bone staples, to determine the most effective (strongest, most stable) wire construct.¹¹⁻²² While understanding the stability

imparted by the whole construct is important, the purpose of our study was to evaluate the role of the wire portion alone, without the confounding factor of K-wire stabilization. Cerclage wires tied to greater tension will resist higher loads before loosening.²³ The tension achieved with different tension band wire configurations is unknown. The first objective of this study was to examine the amount of tension generated during tying of various TB configurations. As load is applied to a TB, it must resist that load and not elongate. Our second objective was to examine the ability of different TB configurations to resist the applied load. We hypothesized that, compared with figure-of-eight configurations with one or two twists, dual interlocking single loop and double loop configurations would generate greater initial tension, resist a greater load at 2 mm of displacement, and better retain resting tension with incremental cyclic loading. Additionally, we hypothesized that the load required to cause 2 mm of displacement (in a monotonic test) and the remaining resting tension after reaching 2 mm of displacement (in a cyclic test) would be positively correlated with the initial tension generated during tying the wire. Determining the load resisted by the wire configuration independent of the K-wire contribution to the construct may provide valuable information for developing improved TB wire designs.

MATERIALS AND METHODS

Trochanteric Osteotomy Model

A trochanteric osteotomy model was designed to evaluate the wire portion of the construct, independent of the contribution of the K-wires. An anatomically correct, solid brass “femur” was milled using a computer model derived from a computed tomography scan of a 30-kg canine right femur. The solid femur model was modified to simulate a greater trochanteric

osteotomy by cutting the trochanter fragment off the “bone” at an angle of 45 degrees to the long axis (Fig. 1). Both cut surfaces were polished to minimize friction as the trochanter fragment moved proximally when loaded. Two 2.4-mm diameter 316LVM stainless steel pins were inserted perpendicular to the “osteotomy” line into the craniolateral and caudolateral aspects of the trochanter fragment. Because the pins were only in the trochanter fragment and did not extend across the osteotomy line into the rest of the “bone,” the trochanter fragment was only constrained by the wire configuration being assessed. To facilitate creation of the TB loops, the exposed pin tips were bent over, and a 2.5-mm diameter hole was drilled transversely through the distal aspect of the proximal metaphysis to serve as the distal anchor for the tension band wire. This hole was positioned 12 mm distal to the distal edge of the osteotomy and 6 mm in from the lateral surface.

To test the TB constructs in the orientation of physiological loading, the femur model was rigidly fixed to a custom jig at an angle of 45° and secured in a servohydraulic load frame (858 Mini Bionix II, MTS Systems Corporation, Eden Prairie, MN) (Fig. 1). To apply loads to the greater trochanter fragment a stainless steel eyebolt (#210 Everbuilt, Home Depot) was fitted at the fragment apex to mimic the attachment site of the gluteal tendon. The eyebolt link was connected to a steel chain (3410T74, 1225 kg load capacity, McMaster-Carr, Elmhurst, IL) using a D-Shackle (3824T71, McMaster-Carr). The top end of the chain was connected to the 15-kN load cell using another D-Shackle. The load cell was mounted to the linear actuator of the load frame. Prior to tying each specimen, the actuator was adjusted so that the trochanter fragment was in its anatomic position. To facilitate wire placement, the trochanter fragment was temporarily stabilized with a small pin that passed through the fragment into the parent “bone.” Once the wire was positioned, and prior to tightening, the temporary pin was removed.

Tension Band Configurations

Four tension band configurations were tested (Fig. 2), including the standard figure-of-eight with one twist (OT), a figure-of-eight with two twists (TT), the dual interlocking single loop construct (DISL), and a double loop (DL) construct modified from a previously published one.¹³ All constructs were formed with 316L, 1.0-mm orthopaedic wire (18 gauge, IMEX Veterinary, Longview, TX). The OT configuration was formed by passing the wire through the distal anchor hole, crossing the lateral aspect of the femur model, wrapping around the pins, and connecting back to its other end with a twist knot (Fig. 2A). The TT configuration was formed in a similar manner, except that a loop was formed in the wire that passed from the anchor hole to the pins (Fig. 2B). This loop, and the joined wire ends, were twisted, resulting in both portions of the figure-of-eight being tightened.

The DISL configuration employed two wires, each with a 2-mm loop formed at one end (Fig. 2C). One wire (I) was passed through the distal anchor hole and the loop positioned adjacent to the hole, on the cranial surface. The second wire (II) was passed around the pins, with the loop beside the more cranial pin. The free end of the distal wire was passed across the lateral aspect of the femur model and through the loop of the proximal wire. The free end of the proximal wire was passed across the lateral aspect of the femur model and through the loop of the distal wire. The two free ends were introduced into a wire tightener (Item 391.21, DePuy Synthes Vet, West Chester, PA) and secured to the cranks. The cranks were turned simultaneously to tighten the wires until the operator assessed appropriate tightness. While holding that tension, the wire tightener was twisted to lock the ends to each other.

The DL configuration was formed from a length of wire with a 2-mm loop formed at its midpoint (Fig. 2D). This loop was positioned between the pins and the free ends passed around the pins, crossed over the lateral aspect of the femur model, passed through the distal anchor hole, and brought back, and through, the loop. The ends were introduced into a wire tightener, secured to the cranks, and the wires tightened simultaneously until the operator assessed appropriate tightness. While maintaining crank tension, the wire tightener was bent over. The cranks were turned in reverse to release 1 cm of wire, which was bent flat and then cut.

Mechanical Testing

For each test, the trochanter fragment was moved to a “reduced” position, and the load cell output was set to zero. The wire constructs were tied, and once the knot was complete and the wire ends cut, the initial *resting tension* was recorded. To examine the effectiveness of the twist-and-lay technique used for the OT and TT constructs, the tension generated during the tying process (*tying tension*) was recorded for these configurations prior to completing the final folding or setting of the knot.

Monotonic tests were performed on one set of wires (n=8 per configuration), which were distracted to failure at an actuator speed of 50 mm/min. Time, force, and displacement data were recorded at 100 Hz (TestStar™ IIs, version 3.5C, MTS Systems Corp.). The mechanism by which the wire elongated was noted from direct observation and video recordings of the tests. All data processing was performed using MATLAB® (The MathWorks, Inc., Natick, MA). Force-displacement curves were generated, and the *clinical failure load* was determined as the force measured at 2 mm of displacement.

Cyclic tests were performed on a second set of wires (n=8 per configuration) using an incrementally increasing loading protocol to evaluate loosening.²³ Each construct was distracted under load control at an actuator speed of 50 mm/min. The first applied load was 50 N, and the load was increased incrementally by 25 N until the applied load at which 2 mm of displacement was reached, which would be the equivalent of clinical failure. During each cycle, the constructs were distracted up to the desired load and then returned to the “zero” position. Time, force, and displacement data were recorded at 50 Hz throughout testing. The following parameters were calculated using MATLAB®: maximum displacement reached during each cycle, resting tension remaining in the wire at the end of each cycle, failure load (load at 2 mm of displacement), and tension loss between the initial and final resting tensions. The final resting tension was recorded at the end of the cycle where 2 mm of displacement was achieved.

Statistical Analyses

For the monotonic loading data, differences among the four configurations were examined for the resting tension and failure load at 2 mm of displacement using one-way ANOVAs with Tukey adjustments for multiple comparisons. The twist-and-lay effectiveness was examined for the OT and TT figure-of-eight constructs by comparing the resting tension with the tying tension using paired t-tests. The relationship between failure load and resting tension was determined with linear correlation analysis, and the Pearson correlation coefficient was calculated. For the incremental cyclic loading data, configuration differences were assessed for the initial resting tension, final resting tension, % tension loss, and failure load at 2 mm of displacement using one-way ANOVAs with Tukey post-hoc comparisons. The relationship between the final and initial resting tensions was determined with linear correlation analysis, and

the Pearson correlation coefficient was calculated. A significance level of 0.05 was used for all analyses (GraphPad Prism[®] 6, La Jolla, CA).

RESULTS

During the monotonic tests, none of the wires broke before reaching 2 mm of displacement. By visual inspection, the DL initially underwent slight wire stretch prior to the two bent wires lifting up as load continued to be applied. The DISL initially elongated via stretching of each end loop. For both figure-of-eight constructs, after a brief period of initial stretch or flattening, elongation occurred by untwisting of the knot(s).

Greater initial resting tension was generated with the DL configuration (128 ± 24 N) than the DISL (46 ± 5 N), TT (56 ± 12 N) and ST (36 ± 9 N) configurations ($p < 0.0001$ for all, Fig. 3). The resting tension of the DISL was not significantly different than that of the TT or OT, but it was greater in the TT than in the OT ($p = 0.041$). The twist-and-lay method of tying was effective for the TT configuration, increasing the tension by 36% after bending over the twisted wire (56 ± 12 N vs. 42 ± 6 N, $p = 0.020$). The tension in the OT construct did not change significantly with the twist-and-lay method (36 ± 9 N vs. 33 ± 5 N, $p = 0.38$). The failure load at 2 mm of displacement was greater for the DL (402 ± 39 N) than the DISL (206 ± 14 N), TT (199 ± 20 N), and OT (165 ± 15 N) configurations ($p < 0.0001$ for all, Fig. 4). The failure load of the DISL was not significantly different than that of the TT configuration, but both DISL and TT failure load was greater than that of the OT configuration ($p = 0.0092$ and 0.039 , respectively). The failure load was linearly correlated with the resting tension (slope = 2.3 ± 0.15 , $r = 0.945$, $p < 0.0001$).

For the incremental cyclic tests, the modes of failure were the same as described for the monotonic tests. By the end of the 11th cycle (300 N), all of the DISL, TT, and OT samples had reached the 2-mm failure point, but only one DL sample had failed, and the remaining DL samples maintained 19% of their initial resting tension (Fig. 5). Similar to monotonic loading, the DL construct had higher failure loads at 2 mm (333 ± 48 N) than the DISL (247 ± 35 N, $p = 0.0003$), TT (229 ± 25 N, $p < 0.0001$), and OT (217 ± 30 N, $p < 0.0001$) constructs (Fig. 6). At failure, which occurred at different cycles for each sample, the final resting tension was significantly higher in the DL (11 ± 3 N) than in the DISL (1.0 ± 1.9 N), TT (2.7 ± 3.7 N), and OT (1.4 ± 3.5 N) configuration ($p < 0.0001$ for all, Fig. 7). The tension loss between the initial and final resting tensions was significantly lower for the DL ($89 \pm 3\%$) than for the DISL ($99 \pm 2\%$, $p = 0.046$) but was not significantly different than the TT ($95 \pm 8\%$) or OT ($97 \pm 11\%$) configurations. The final resting tension was linearly correlated with the initial resting tension (slope = 0.11 ± 0.019 , $r = 0.736$, $p < 0.0001$).

DISCUSSION

As we hypothesized, compared with the figure-of-eight configurations using both one and two twists, the double loop tension band wiring construct generated greater initial resting tension, resisted a higher load before 2 mm of displacement, and maintained a greater percentage of the resting tension under incremental cyclic loading. The failure load was highly correlated with the initial resting tension, so the aspects of the knot and tying technique that contributed to a relatively higher resting tension in the DL configuration also resulted in a better ability to resist the applied load. The greater initial resting tension with the DL results primarily from the use of a wire tightener to tighten the construct. The cranks enable the wire to be tensioned to its yield

load and, while some of that tension is lost as the arms are folded over, much is retained, resulting in the higher loads measured. In contrast, in the twist knots the wire is tightened by wrapping the strands around one another and rotating the gripping instrument, which appears less efficient at retaining tension in the wire. The ability to resist load in these constructs relates to the mode by which the knots are “undone;” the twist styles experience untwisting, and the arms of the loop styles unbend. Because the DL configuration has two arms, it can better resist distraction and thus sustains higher loads before loosening to the point of failure. However, given that the knot or fold is the weak point of the system, this finding also suggests that more force is required to unbend two arms than to untwist two wires wrapped around each other as is present in the other three constructs.

Contrary to our hypothesis, the DISL construct did not achieve a higher initial resting tension than the OT or TT, although it did resist a higher load before 2 mm of displacement than the OT construct. Similarly, the DISL construct did not maintain the resting tension under cyclic loading any better than the one or two twist constructs. Tightening the more complex DISL configuration is more difficult than the other configurations in this study, even with the use of the wire tightener, which may explain the inability to achieve a higher resting tension than with the figure-of-eight constructs. When loaded, the loops in the DISL elongated first, resulting in yield and elongation of the construct at lower loads. After this initial elongation, however, the configuration was stiffer and resisted higher loads, although this generally occurred after the clinical failure point of 2 mm displacement. Therefore, using clinically relevant criteria, the DISL construct was no more effective than the OT or TT constructs and was more difficult to form and tie.

The four configurations chosen were based on more commonly used patterns, as well as studies indicating increased strength of the double loop and dual interlocking single loop. With two wires involved in the tightening process, the double loop generates greater static tension and a higher yield load,²⁴ and it can resist higher loads at 2 mm of displacement,¹³ when compared to single loop or twist cerclage. Because this technique requires the use of a tensioner and thus is potentially more difficult, we also included the commonly used figure-of-eight patterns in the study, not only to evaluate them against the DL and DISL but also to compare them to each other in regard to utilizing twists on one side of the figure-of-eight versus both sides. In a human cadaver study evaluating five tension band configurations for reduction of an olecranon osteotomy, the figure-of-eight tension band wiring using two tightening knots was more effective in preventing motion under forces involved in active mobilization of the elbow immediately after operation compared to a figure-of-eight with one twist.¹⁴ In our study, the construct with two twists similarly resisted movement better than the one with one twist and thus was able to achieve a 21% higher force before failure at 2 mm (199 N vs. 165 N).

When initially evaluating these configurations, we noted several factors involved in executing their placement that were important for the performance of the tension band wiring: 1) using a small loop end of the wire, 2) minimizing laxity in the wire during tying, and 3) holding tension on the cranks of the wire tightener throughout the wire tying process. For wire configurations utilizing a formed loop, stretch of the loop was the first response to load; therefore, consistently making the loop as small as possible was important in producing the strongest DISL and DL constructs. These findings were similar to a previous study stating that constructs failed by knots untwisting or knots stretching and elongating the loops,¹³ further supporting the importance of forming the loop end of the wire as small as possible.

When placing the wire through the metaphyseal hole and looping around the trochanter fragment, we found that maintaining tension on the wire and a tight press fit along the fragment to eliminate any laxity in the wire were important to avoid more immediate loss of stiffness when load was applied. For the figure-of-eight configurations, we found that pulling up on the wire during the final twist-and-lay technique was also important in maintaining the wire tension, and in the case of the TT construct actually increased the wire tension by 36%. For the double loop configuration in this study, we held tension by maintaining pressure on the cranks of the wire tightener while bending over the wire, as previously described,²³ which helped achieve the 2.3-3.5 times greater initial tension for the DL compared with the others, resulting in 2.0-2.4 times greater strength (force at 2 mm). Although the different configurations had significant differences in resistance to load in this study, following these basic practices in wire tying will help produce the most secure construct for any given configuration.

One unique aspect of this study is the analysis of the tying process to help understand the differences between the different wire configurations in terms of the separate tightening and securing processes during tying. The twist-and-lay technique was able to maintain (OT) or even increase by 36% (TT) the wire tension during the securing process. After the twist was formed to a perceived tightness of just less than optimal, the knot was pulled up and an additional half twist was formed while simultaneously laying it over. The twist-and-lay technique is preferred over the technique of pushing the completed twist flat, which results in greater tension loss during the flattening process.²⁵ The higher percent increase in the construct with two twists can be explained by the fact that both loops of the figure-of-eight are individually tightened for an even distribution of tension, whereas in the construct with one twist, only a single location is twisted to tighten the entire figure-of-eight, which impairs an even distribution of tension. The advantage

of the figure-of-eight with two twists over just one twist is further supported by the fact that the TT construct has a higher resting tension and resists more load before failure at 2 mm displacement. Nevertheless, the double loop was the best TB configuration in this study, primarily owing to its substantially higher resting tension than the other three constructs. Achieving as high a resting tension as possible is important, because the failure load is highly correlated with ($r = 0.945$) and scales with the resting tension by a factor of 2.3.

The femur model and setup for testing the TB configurations in this study were designed to be anatomically correct and simulate physiological loading on the greater trochanter during gait yet also isolate the performance of the wiring portion of the construct and remove the contributions of K-wire stabilization and bone stiffness. In previous studies using bone models, the materials used to simulate bone were more compliant, such as Delrin® bar models or wooden patella models,^{11,12,20,21} introducing undesired compliance within the testing structure that could potentially confound the mechanical property measurements of the constructs alone. Similar to our study, some previous studies used anatomical loading, but they inserted K-wires across the fracture gap for stability and thus did not isolate the performance of the wiring configurations under loading.^{11-14,16,18-22,26,27} Other previous studies isolated the wiring configurations but did not perform anatomical loading.^{23,28-31} To our knowledge our study is the first to incorporate all of these aspects, thereby providing an isolated comparison of various tension band wiring configurations without contributions from other parts of the bone and stabilization system.

Conclusions/Limitations

Our results indicate that the double loop configuration offers the greatest initial tension and resistance to load. The two twist figure-of-eight was superior in initial tension and load

resistance when compared to the one twist figure-of-eight and thus should still be considered intra-operatively if a tensioning device is not available to aid in tying the double loop configuration. Our model and testing setup provided an effective means for isolating the performance of the wiring and comparing it across different configurations. While our bone model did not have the same material properties as bone, the ability to test all wires on the same construct minimized the variability within groups. Because our model did not include the K-wires that bridge the fracture, the wire configurations could be evaluated independently of that portion of the tension band construct. The forces measured are, therefore, not representative of the forces that would be resisted by a complete tension band fixation. This study not only evaluated the behavior of the wire configurations during tying and a single load application to failure, as might occur with an inadvertent over-exertion by a patient, it also assessed how the resting tension is lost for these configurations with different magnitudes of repeated loading. This study did not examine the fatigue properties under low-load cyclic loading, which may be useful for fully understanding the *in vivo* performance of these constructs. While the current study used a canine femur model to evaluate tension band wiring, determining the strongest configuration to resist applied loads is important, regardless of the species or anatomical location. This study helps elucidate stronger configurations to dictate appropriate intra-operative decision-making when a fracture or osteotomy requires fixation in a location where large tensile forces are applied to a fragment.

ACKNOWLEDGMENTS

The authors thank Dr. Timothy Horn for fabrication of the brass femur model, David Lee and Seth Steele-Pardue for assistance with modifications made to the femur model, Austin Murray

for initial design work on the custom jig used in mechanical testing, and David Buffaloe for help with jig fabrication.

REFERENCES

1. Weber BG, Vasey H. 1963. [Osteosynthesis in Olecranon Fractures]. *Z Unfallmed Berufskr* 56:90-96.
2. Wolfgang G, Burke F, Bush D, et al. 1987. Surgical treatment of displaced olecranon fractures by tension band wiring technique. *Clin Orthop Relat Res*:192-204.
3. Denny HR. 1975. The use of the wire tension band in the treatment of fractures in the dog. *J Small Anim Pract* 16:173-183.
4. Gibbons SE, Macias C, Tonzing MA, et al. 2006. Patellar luxation in 70 large breed dogs. *J Small Anim Pract* 47:3-9.
5. Halling KB, Lewis DD, Cross AR, et al. 2002. Complication rate and factors affecting outcome of olecranon osteotomies repaired with pin and tension-band fixation in dogs. *Can Vet J* 43:528-534.
6. Hauptman JOE, Butler HC. 1979. Effect of Osteotomy of the Greater Trochanter with Tension Band Fixation on Femoral Conformation in Beagle Dogs. *Vet Surg* 8:13-18.
7. Ostrum RF, Litsky AS. 1992. Tension band fixation of medial malleolus fractures. *J Orthop Trauma* 6:464-468.
8. Palmer RH, Aron DN, Chambers JN. 1988. A combined tension band and lag screw technique for fixation of olecranon osteotomies. *Vet Surg* 17:328-332.
9. Parkinson DE, Joseph R, Edelman R. 1988. Biomechanical principles of tension band wiring applied to fractures of the distal fibula and fifth metatarsal base. *J Foot Surg* 27:149-156.

- 383 10. Macko D, Szabo RM. 1985. Complications of tension-band wiring of olecranon fractures. J
384 Bone Joint Surg Am 67:1396-1401.
- 385 11. Neat B, Kowaleski MP, Litsky AS, et al. 2006. The effects of wire diameter and an
386 additional lateral wire on pin and tension-band fixation subjected to cyclic loads. Vet Comp
387 Orthop Traumatol 19:213-218.
- 388 12. Neat BC, Kowaleski MP, Litsky AS, et al. 2006. Mechanical evaluation of pin and tension-
389 band wire factors in an olecranon osteotomy model. Vet Surg 35:398-405.
- 390 13. Grafinger MS, Roe SC, Spodnick G, et al. 2007. Biomechanical comparison of dual
391 interlocking single loop and double loop tension band techniques to the classic AO tension
392 band technique for repair of olecranon osteotomies in dogs. Vet Surg 36:141-148.
- 393 14. Fyfe IS, Mossad MM, Holdsworth BJ. 1985. Methods of fixation of olecranon fractures. An
394 experimental mechanical study. J Bone Joint Surg Br 67:367-372.
- 395 15. Halling KB, Lewis DD, Cross AR, et al. 2003. Biomechanical comparison of a circular
396 external skeletal fixator construct to pin and tension band wire fixation for the stabilization of
397 olecranon osteotomies in dogs: a cadaveric study. Vet Surg 32:324-335.
- 398 16. Hutchinson DT, Horwitz DS, Ha G, et al. 2003. Cyclic loading of olecranon fracture fixation
399 constructs. J Bone Joint Surg Am 85-A:831-837.
- 400 17. Mullett JH, Shannon F, Noel J, et al. 2000. K-wire position in tension band wiring of the
401 olecranon - a comparison of two techniques. Injury 31:427-431.
- 402 18. Reising K, Konstantinidis L, Helwig P, et al. 2014. Biomechanical testing of an innovative
403 fixation procedure to stabilize olecranon osteotomy. Proc Inst Mech Eng H 228:1146-1153.
- 404 19. Wu CC, Tai CL, Shih CH. 2000. Biomechanical comparison for different configurations of
405 tension band wiring techniques in treating an olecranon fracture. J Trauma 48:1063-1067.

- 406 20. Ali M, Kuiper J, John J. 2016. Biomechanical analysis of tension band wiring (TBW) of
407 transverse fractures of patella. Chinese journal of traumatology = Zhonghua chuang shang za
408 zhi 19:255-258.
- 409 21. John J, Wagner WW, Kuiper JH. 2007. Tension-band wiring of transverse fractures of
410 patella. The effect of site of wire twists and orientation of stainless steel wire loop: a
411 biomechanical investigation. Int Orthop 31:703-707.
- 412 22. Kozin SH, Berglund LJ, Cooney WP, et al. 1996. Biomechanical analysis of tension band
413 fixation for olecranon fracture treatment. Journal of shoulder and elbow surgery 5:442-448.
- 414 23. Roe SC. 1997. Mechanical characteristics and comparisons of cerclage wires: introduction of
415 the double-wrap and loop/twist tying methods. Vet Surg 26:310-316.
- 416 24. Blass CE, Piermattei DL, Withrow SJ, et al. 1986. Static and Dynamic Cerclage Wire
417 Analysis. Vet Surg 15:181-184.
- 418 25. Wähnert D, Lenz M, Schlegel U, et al. 2011. Cerclage handling for improved fracture
419 treatment. A biomechanical study on the twisting procedure. Acta Chir Orthop Traumatol
420 Cech 78:208-214.
- 421 26. Gruszka D, Arand C, Nowak T, et al. 2015. Olecranon tension plating or olecranon tension
422 band wiring? A comparative biomechanical study. Int Orthop 39:955-960.
- 423 27. Parent S, Wedemeyer M, Mahar AT, et al. 2008. Displaced olecranon fractures in children: a
424 biomechanical analysis of fixation methods. Journal of pediatric orthopedics 28:147-151.
- 425 28. Bostrom MP, Asnis SE, Ernberg JJ, et al. 1994. Fatigue testing of cerclage stainless steel
426 wire fixation. J Orthop Trauma 8:422-428.
- 427 29. Lenz M, Perren SM, Richards RG, et al. 2013. Biomechanical performance of different cable
428 and wire cerclage configurations. Int Orthop 37:125-130.

- 429 30. Meyer DC, Ramseier LE, Lajtai G, et al. 2003. A new method for cerclage wire fixation to
430 maximal pre-tension with minimal elongation to failure. Clin Biomech (Bristol, Avon)
431 18:975-980.
- 432 31. Schultz RS, Boger JW, Dunn HK. 1985. Strength of stainless steel surgical wire in various
433 fixation modes. Clin Orthop Relat Res:304-307.
- 434

FIGURE LEGENDS

Figure 1. Solid brass right femur model with a 45° osteotomy, rigidly mounted in custom jig for mechanical testing of tension band configurations. Loads were applied via a steel chain at an angle of 45° to mimic gluteal tendon loading.

Figure 2. Tension band wiring configurations on the right femur model with a 45° osteotomy: A) Figure-of-eight with one twist (OT), B) figure-of-eight with two twists (TT), C) dual interlocking single loop (DISL), and D) double loop (DL). The DISL construct was formed with two wires (I,II).

Figure 3. Monotonic test resting tension for the four tension band configurations. Mean \pm standard deviation. ** $p < 0.0001$ for DL vs. DISL, TT, and OT. * $p = 0.041$ for TT vs. OT.

Figure 4. Monotonic test failure load at 2 mm of displacement for the four tension band configurations. Mean \pm standard deviation. ** $p < 0.0001$ for DL vs. DISL, TT, and OT. * $p = 0.00092$ for DISL vs. OT and $p = 0.039$ for TT vs. OT.

Figure 5. Cyclic test resting tension for the four tension band configurations over incremental loading cycles. Mean \pm standard deviation at each cycle until failure.

Figure 6. Cyclic test failure load at 2 mm of displacement for the four tension band configurations. Mean \pm standard deviation. ** $p = 0.0003$ for DL vs. DISL and $p < 0.0001$ for DL vs. TT and OT.

Figure 7. Cyclic test final resting tension (after failure at 2 mm was reached) for the four tension band configurations. Mean \pm standard deviation. ** $p < 0.0001$ for DL vs. DISL, TT, and OT.



Figure 1. Solid brass right femur model with a 45° osteotomy, rigidly mounted in custom jig for mechanical testing of tension band configurations. Loads were applied via a steel chain at an angle of 45° to mimic gluteal tendon loading.

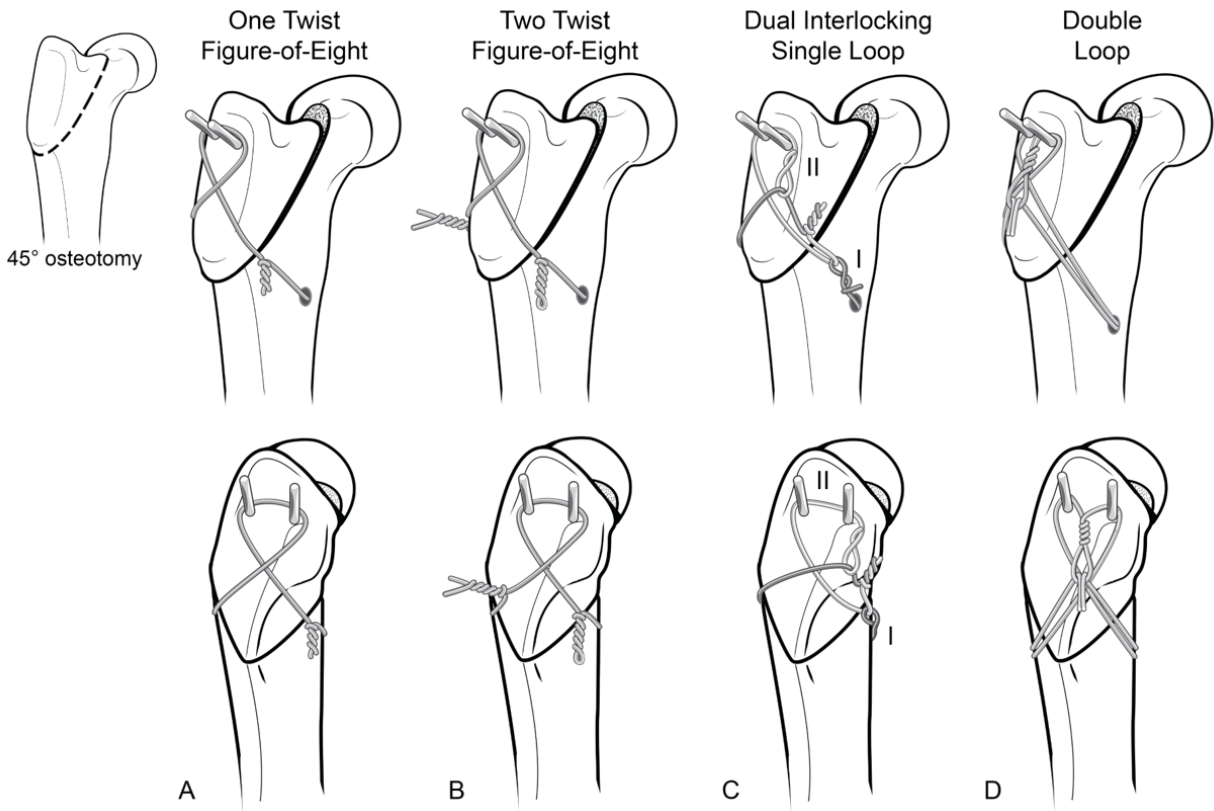


Figure 2. Tension band wiring configurations on the right femur model with a 45° osteotomy: A) Figure-of-eight with one twist (OT), B) figure-of-eight with two twists (TT), C) dual interlocking single loop (DISL), and D) double loop (DL). The DISL construct was formed with two wires (I,II).

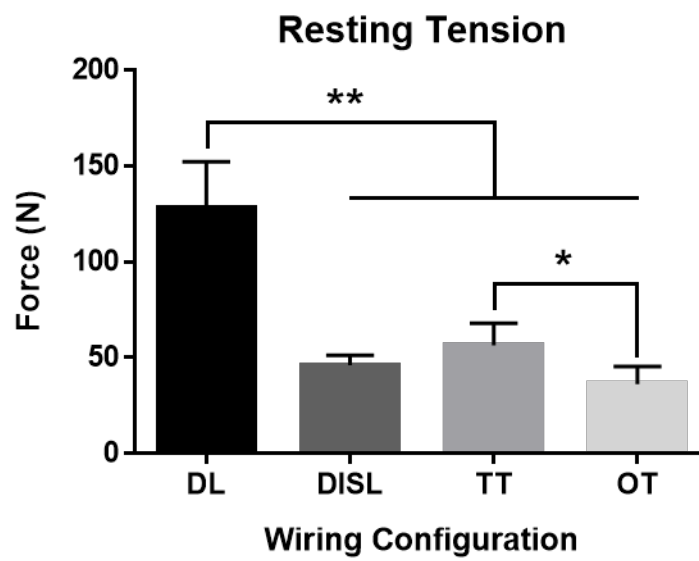


Figure 3. Monotonic test resting tension for the four tension band configurations. Mean \pm standard deviation. ** $p < 0.0001$ for DL vs. DISL, TT, and OT. * $p = 0.041$ for TT vs. OT.

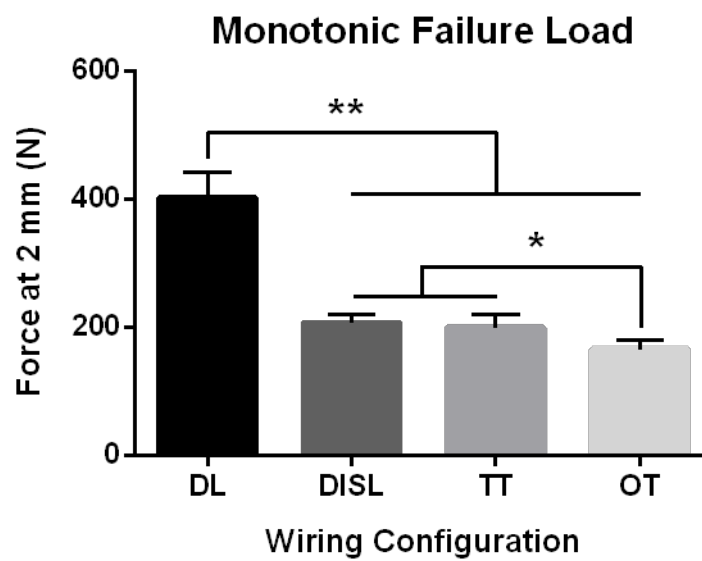


Figure 4. Monotonic test failure load at 2 mm of displacement for the four tension band configurations. Mean \pm standard deviation. **p < 0.0001 for DL vs. DISL, TT, and OT. *p = 0.00092 for DISL vs. OT and p = 0.039 for TT vs. OT.

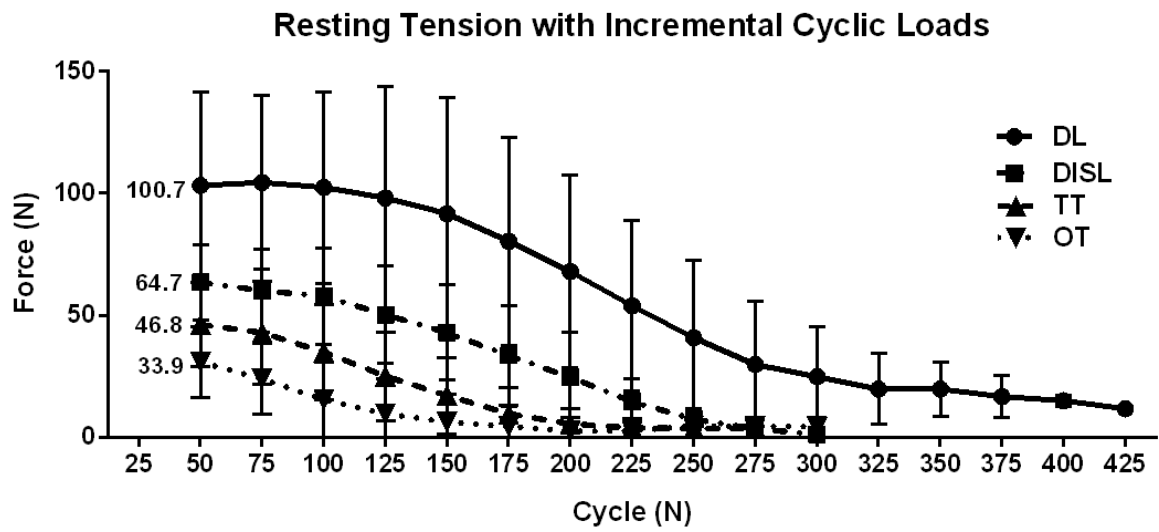


Figure 5. Cyclic test resting tension for the four tension band configurations over incremental loading cycles. Mean \pm standard deviation at each cycle until failure.

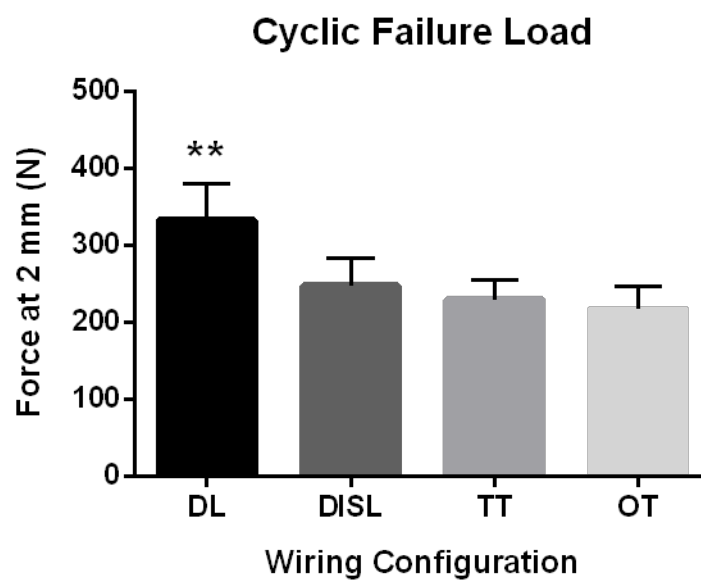


Figure 6. Cyclic test failure load at 2 mm of displacement for the four tension band configurations. Mean \pm standard deviation. ** $p = 0.0003$ for DL vs. DISL and $p < 0.0001$ for DL vs. TT and OT.

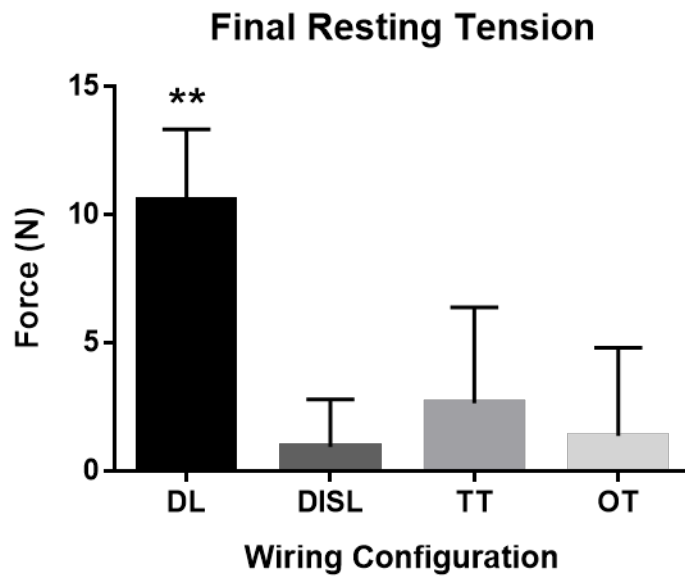


Figure 7. Cyclic test final resting tension (after failure at 2 mm was reached) for the four tension band configurations. Mean \pm standard deviation. ** $p < 0.0001$ for DL vs. DISL, TT, and OT.